Azimuthally Polarized, Circular Colloidal Quantum Dot Laser Beam Enabled by a Concentric Grating

Yuan Gao,[†] Landobasa Y. M. Tobing,[†] Aurélien Kiffer,[‡] Dao Hua Zhang,[†] Cuong Dang,[†,‡,] Hilmi Volkan Demir[†,§,#,*]*

[†]LUMINOUS! Center of Excellence for Semiconductor Lighting and Displays, Satellite Research Centre, Centre for Optoelectronics and Biophotonics, The Photonics Institute, School of Electrical and Electronic Engineering and The Photonics Institute, Nanyang Technological University, 50 Nanyang Avenue, 639798, Singapore.

[‡]CNRS International NTU Thales Research Alliance (CINTRA), Research Techno Plaza, 50 Nanyang Drive, Border X Block, 637553, Singapore.

[§]Division of Physics and Applied Physics, School of Physical and Mathematical Sciences, Nanyang Technological University, 21 Nanyang Link, 637371, Singapore.

[#]Department of Electrical and Electronics Engineering and Department of Physics, UNAM – Institute of Materials Science and Nanotechnology, Bilkent University, Bilkent, Ankara, Turkey.

ABSTRACT: Since the optical gain was observed from colloidal quantum dots (CQDs), research on CQD lasing has been focused on the CQDs themselves as gain materials and their coupling with optical resonators. Combining the advantages of a CQD gain medium and optical microcavity in a laser device is desirable. Here, we show concentric circular Bragg gratings intimately incorporating CdSe/CdZnS/ZnS gradient shell CQDs. Because of the strong circularly symmetric optical confinement in two dimensions, the output beam CQD-based circular grating distributed feedback (DFB) laser is found to be highly spatially coherent and azimuthally polarized with a donut-like cross section. We also observe the strong modification of the photoluminescence spectrum by the grating structures, which is associated with modification of optical density of states. This effect confirmed the high quality of the resonator that we fabricated and the spectral overlap between the optical transitions of the emitter and resonance of the cavity. Single mode lasing has been achieved under a quasi-continuous pumping regime; meanwhile, the position of the lasing mode can be conveniently tuned via adjusting the thickness of the CQD layer. Moreover, a unidirectional output beam can be observed as a bright circular spot on a screen without any collimation optics, presenting a direct proof of its high spatial coherence.

Keywords: colloidal quantum dot, lasing, circular grating, azimuthal polarization, DFB

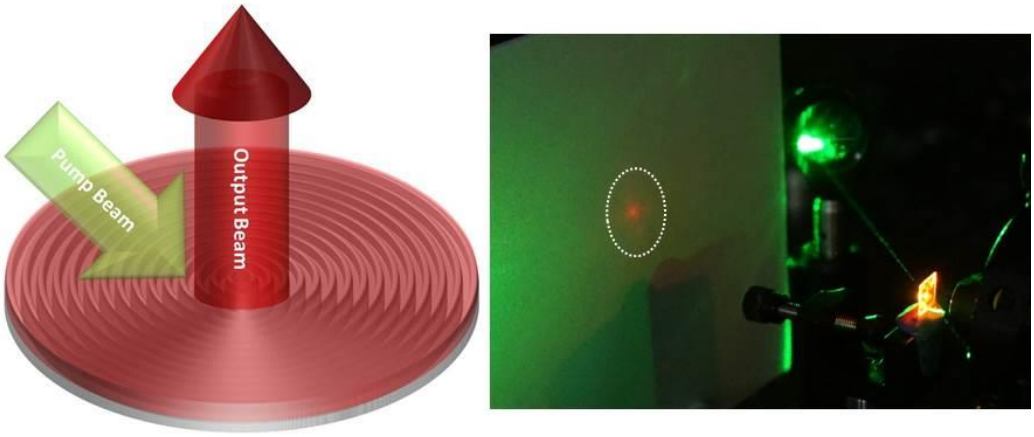

Colloidal quantum dots (CQDs), which are regarded as "nanoscience building blocks",[1] have attracted a lot of research interests globally for more than three decades.[2] One of the most intriguing properties of semiconductor CQDs is that their electronic structures are tunable flexibly via adjusting their size, chemical composition, morphology, or adopting heterostructures.[3] As a result, the light emission from the semiconductor CQDs can be designed to cover the entire visible spectral range with a high quantum yield and a narrow linewidth. Moreover, considering their tunable emission wavelength, CQDs are able to bridge the so-called "green gap" in conventional light emitters.[4] Given their unique optical properties, CQDs are very promising in improving the qualities of modern lighting and displays.[5-6]

Due to the so-called quantum confinement effect, the semiconductor CQDs exhibit discrete energy levels, and such discrete energy levels make them applicable to fabrication of thermally stable lasers.[7-8] After Klimov and his colleagues realized CdSe CQD lasing in room temperature in 2000, the research on CQD lasing has been on rising.[7, 9] Single-exciton gain in CQDs has been shown to overcome the Auger process, which is a fundamental problem of CQD lasing.[10-11] Red, green, or blue (RGB) lasing from semiconductor CQDs have been demonstrated by incorporation with various optical feedback configurations, such as Fabry–Pérot cavities,[12-13] Whispering gallery mode (WGM),[14-16] distributed feedback (DFB) lasers,[17-19] and others[20]. However, most of the works did not show the output laser beam from the laser devices, which is a direct evidence of the spatial coherence of lasers.[21] In this work, we show the first account of a highly spatial coherent CQD-based surface-emitting circular grating DFB (CG-DFB) laser.

Conventional one-dimensional (1D) DFB laser can provide optical feedbacks in only one direction. Therefore, the surface-out-coupling beam has different divergences in the orientations along and normal to the gratings. This problem, in essence, can be addressed by fabricating the gratings in a circular fashion.[22] Because of the strong and in-plane symmetric confinement of the resonant mode, the CG-DFB lasers exhibit low operation threshold and low divergent circularly symmetric output beam.[23-24] Moreover, compared with conventional vertical-cavity-surface-emitting lasers (VCSELs), CG-DFB lasers are expected to possess a high output power due to their large in-plane gain area.[24] Thus, the combination of two-dimensional light confinement in CG-DFB and the optical properties of CQDs would make the CQD-based CG-DFB laser an excellent candidate for achieving high power single mode lasers with high Q-factor at any desired wavelength within the visible spectrum.

In this paper, we report the first account of CQD based CG-DFB lasers. A strong modification of the optical density states (DOS) of the CQDs that were coupled with the circular grating was observed, which is confirmed by two proofs. Firstly, a dent, which was associated with the position of the photonic stop band, appeared in the corresponding fluorescence spectrum. Secondly, we showed a prolonged lifetime of the transitions that lie within the stop band. As the sample is optically pumped, single mode lasing peak emerges at the edge of the stop band, where the optical DOS is enhanced. By characterizing the output lasing, we confirmed that the lasing beam is azimuthally polarized and highly directional, which is a direct proof of the spatial coherence of our CQD-based CG-DFB laser. The findings indicate that the proposed microlaser based on the intimate integration of CQDs into a circular Bragg grating is very promising for various photonic applications that require surface normal geometry and good beam quality.

The fabrication of circular Bragg substrate, formed by 250 concentric circular grooves with 376 nm pitch, was carried out by electron beam (e-beam) lithography followed by dry etching. The positive-tone ZEP520A resist was firstly spin coated on 0.5 mm thick quartz substrate at 150 nm thickness, followed by a 30 nm conductive polymer film (ESPACER) for avoiding charging effects during e-beam patterning. The e-beam exposure was carried out at 65 $\mu C/cm^2$ dose range, and the sample was developed in methyl isobutyl ketone (MIBK) at 6 °C for 10 s. The dry etching process was based on 30 sccm CF4 and 30 sccm CHF3 gasses at 150 mT pressure, using 170 W radio frequency (RF) power for 555 s. Then, the resist was removed with Piranha solution (a mixture of concentrated H_2SO_4 and H_2O_2 with a ratio of 3:1). The period of the circular grating is 376 nm. The scanning electron microscopic (SEM) images of the substrate are presented in Fig. 1. A thin layer of poly(3,4-ethylenedioxythiophene) polystyrene sulfonate (PEDOT:PSS) was temporally spin-coated on the quartz substrate surface to increase its electrical conductivity and avoid charging during SEM inspection. As can be seen from the SEM images, the fabricated circular grating was free from defects, and the roughness resulted from the dry etching process are in deep-subwavelength range, suggesting that the as-fabricated circular Bragg gratings are promising for high-quality laser applications. In addition, the quartz circular Bragg substrate can serve as a mold for imprinting the grating pattern onto other flexible substrates.[18, 25-26]

The semiconductor CQDs (CdSe/CdZnS/ZnS core-shell structures) that were deployed as the gain medium were synthesized with one-pot method,[27] as shown in the high-resolution transmission electron microscopy (HRTEM) image in Fig. S1a. The ZnS shells not only increase absorption cross section of CQDs but also ensure a good passivation of the surface defects of the cores. Therefore, the photoluminescence (PL) spectrum of the CdSe/CdZnS/ZnS CQD solution exhibits a narrow line width and Gaussian-like symmetric shape, which can be seen from the Fig. S1b. Meanwhile, the gradient composition shells and the quasi-type-II band alignment make the Auger effect alleviated in such CdSe/CdZnS/ZnS CQDs, which is desirable for achieving low threshold lasing action in CQDs.[28-29] The PL quantum yield (PLQY) for the diluted CdSe/CdZnS/ZnS CQD solution was 0.62, measured with an integrating sphere and excitation of 405 nm laser.

A densely packed and uniform CQD film was prepared by spin-coating a concentrated CdSe/CdZnS/ZnS CQD solution (100 mg/mL) onto the quartz substrate at a rate of 1000 rpm/min. The thickness of the CQDs film was 246.52±6.49 nm, which was characterized with an ellipsometer (VASE VB-250). The sample was pumped at 532 nm by a frequency-doubled Nd:YAG laser with a repetition rate of 60 Hz and pulse width of 0.5 ns. The focused laser

spot was adjusted to cover the entire region of a circular grating pattern, and the spot size was about 4.21×10^{-4} cm^2. The signals were collected vertically to the sample surface by an objective lens and analyzed with a monochromator (ANDOR Shamrock 303i) and a charge-coupled device (CCD) (ANDOR iDus 401); meanwhile, the excitation spot was monitored with a CCD camera (Thorlabs). As shown in Figure 1c, under low excitation energy, the CQDs that were in the circular grating pattern area are brighter than those were outside, which is attribute to the increased surface-vertical light scattering from the circular grating. When the excitation spot located outside the circular gratings, the PL spectrum of the CdZnSeS/ZnS CQD film is shown in Fig. 2a. The PL spectrum exhibits a 2.2 nm red shift compared to that of the diluted solution; this is due to an increased photons reabsorption and energy transfer between the CQDs. As the pumping energy was increased, the amplified spontaneous emission (ASE) peak occurred on the red side of the PL peak of the CdSe/CdZnS/ZnS CQDs, as shown in Figure 2a. The ASE peaks range from 624 nm to 636 nm, and the spiky peaks are results from the random optical feedbacks within the CQDs film (a random laser). The variation of integrated intensity of the ASE peaks as a function of pumping power is plotted in Fig. 2b, which shows a so-called "soft threshold" and a slow intensity building up above the threshold. Such "soft threshold" is a result of a considerable amount spontaneous emission were collected by the detector,[30] and a small amount of ASE scattered vertically to the detector. When the excitation spot was moved to a circular grating pattern and under low excitation energy, the emission spectrum was suddenly changed, if it is compared with that from CQDs outside the gratings, as shown in Fig.2c. The dent in this spectrum illustrates the position of the stop band. The emission within this stop band was suppressed, because of a reduced optical DOS in the stop band. To confirm the existence of the stop band, the fluorescence lifetime of the CdSe/CdZnS/ZnS CQDs on the substrate was measured with a confocal scanning fluorescence lifetime imaging (FLIM) system. The sample was excited by a pulsed laser with a wavelength of 375 nm, repetition rate of 20 MHz, and pulse duration of 100 ps. The lifetime mapping area is around 126 μm by 126 μm, and the lifetime of each pixel within the mapping area has been recorded. The spectral window of the measurement was 626 ± 10 nm, which was corresponding to the stop band of the CG-DFB laser. The distribution of the fluorescence lifetime of CQDs in the lifetime mapping region was located within or outside the circular grating pattern were displayed in Figure 3. According to the histograms, the fluorescence lifetime distribution of the CQDs that coupled to the circular grating was longer than those that were outside the grating. This is because the optical transitions, which lay in the stop band, of the emitters that coupled with the grating were suppressed. Therefore, the circular grating has a strong modification on the optical DOS of the assembly.

In the other hand, at the edge of the stop band, the optical DOS could be enhanced.[31] As the CQDs coupled with the circular grating were pumped with a higher energy, a sharp lasing peak (634.9 nm) appeared at longer wavelength edge of the stop band. The optical DOS was high at the band edge, resulting in the low group velocity. Therefore, the optical transitions were more favored, and the photons underwent a high optical gain at the stop band edge.[32] The Q factor of this single mode lasing, deduced by $\lambda/\delta\lambda$, is at least 2531 (the determination of the Q factor is limited by the resolution, 0.26 nm at 635 nm, of the spectrometer that we employed). The lasing threshold was two orders lower than the ASE threshold of CQDs that were outside the circular grating. This is because the circular Bragg gratings provided a strong two-dimensional confinement in the waveguide and photons that were propagating in the waveguide can only be coupled to one optical mode. Moreover, considering the pulse width

(0.5 ns) of the laser for optical pumping, which is much longer compared to the time of Auger recombination, our CQD-CG-DFB laser can work under a quasi-continuous wave pumping condition.[9, 19] The power efficiency of our demonstrated CQD-based CG-DFB laser is 0.15%. The output intensity maintained after running continuously for 2 hours under pumping of 183 $\mu J/cm^2$.

The quartz circular Bragg grating substrate is reusable. After the spin-coated layer was rinsed away, and the substrate was cleaned thoroughly by immersing in Piranha solution, a thinner CQD film with a thickness of 203.18±2.88 nm was prepared via spin-coating at a spin rate of 1500 rpm/min. As evident from Fig. 2e, the PL emission of CQDs that lies on the grating differed from that of normal CQDs as well. The position of the modification of the spectrum was blue shifted to the wavelength of around 620 nm. Given the refractive index of CQD thin film (n=1.87, determined via the ellipsometer) is significantly higher than that of quartz grating substrate (n=1.5), the effective refractive index of the laser structure is decreased when CQD film thickness reduces. Therefore, the position of the stop band moved to a shorter wavelength.[18-19] A single mode lasing peak emerged at 624.9 nm, and the corresponding Q factor is at least 2546. The power transfer function is plotted in Figure 2f, and the lasing threshold is comparable to that of the thick CQDs film. Therefore, the emission wavelength of the CQD based CG-DFB laser can be readily tuned within the gain profile merely by a simple adjustment of the CQD layer thickness.

The far-field radiation pattern of the CQD-CG-DFB laser was monitored by a microscope and a CCD camera. As shown in the Figure 4a, at the very center of the far-field pattern, there was a dim spot. Such zero electric field at the center was resulted from the cylindrical boundary condition and the azimuthally polarized emission from the CG-DFB laser.[26, 33-34] The polarization of the emission was analyzed by a polarizer before the CCD camera. The variations of the far-field radiation images as a function of the orientation of polarizer axis are shown in Figure 4b, which perfectly illustrated the azimuthally polarized nature of the laser action from the CQD-CG-DFB laser. Thus, both the zero field at the beam center and the polarization dependent far-field radiation patterns clearly confirm that the out-coupled beam possesses the azimuthal polarization.

Although CQDs lasing has been reported in various laser schemes, only a few of them demonstrated an out-coupled lasing beam, which directly proves the spatial coherence of a laser.[21 21] Due to the circularly symmetric nature of the light confinement, in addition to the light out-coupling via surface-normal second order scattering, the out-coupled beam from the CG-DFB has a circular cross section and is expected to be highly unidirectional. In Figure 5a, a viewing screen was placed behind the CQDs-CG-DFB laser without lens or mirror to focus or collimate the output laser beam. When the CQD-CG-DFB was pumped above its lasing threshold, a bright circular light spot can be seen on the viewing screen (Figure 5b). This demonstrates that our CQD-CG-DFB laser exhibits an excellent spatial coherence, which is advantageous for a laser scheme to be practical.

In this work, we have demonstrated, for the first time, a semiconductor NC-based CG-DFB laser that has a significant modification on the optical DOS of the semiconductor NC emitters and a highly spatially coherent output beam. We coupled a uniform NC layer with the concentric circular Bragg grating of 376 nm pitch, and observed the modifications of emission spectra of CQDs at the grating region indicating the position of the stop band and the enhanced DOS at the band edge. At increased the pump energy, a sharp single mode

lasing peak emerged at the edge of the stop band. For the reason of cylindrical boundary condition that is associated with the circularly symmetric geometry of the CQD-GC-DFB laser, the output beam is azimuthally polarized with zero amplitude at the very center at the emission direction normal to the device surface. The combination of strong two-dimensional light confinement and single mode lasing have led to the dramatic reduction of the lasing threshold by two orders of magnitude. The high directionality of the laser is also demonstrated by projecting the output beam onto the screen without employing any optical components for focusing or collimating purposes. In light of its surface-normal emission, low lasing threshold, single mode lasing operation, circular beam cross section, azimuthal polarization and high spatial coherence, along with the unique optical properties of CQDs, the CQD-CG-DFB laser can find its promising applications in various fields such as displays, lighting, photonic circuits, and high power lasers.

AUTHOR INFORMATION

Corresponding Author:

*E-mail: hcdang@ntu.edu.sg, and hvdemir@ntu.edu.sg

Notes

The authors declare no competing financial interest.

ACKNOWLEDGEMENTS

The authors would like to thank the financial support from Singapore National Research Foundation under NRF-NRFI2016-08, the Singapore Agency for Science, Technology and Research (A*STAR) SERC Pharos Program under Grant No. 152 73 00025, NTU start-up grant and AcRF Tier1 grant RG70/15 from Ministry of Education. The authors also acknowledged the financial support from Ministry of Education (RG86/13), Economic Development Board (NRF2013SAS-SRP001-019) and Asian Office of Aerospace Research and Development (FA2386-14-1-0013). The transmission electron microscopy imaging was performed at the Facility for Analysis, Characterization, Testing and Simulation (FACTS) at Nanyang Technological University, Singapore.

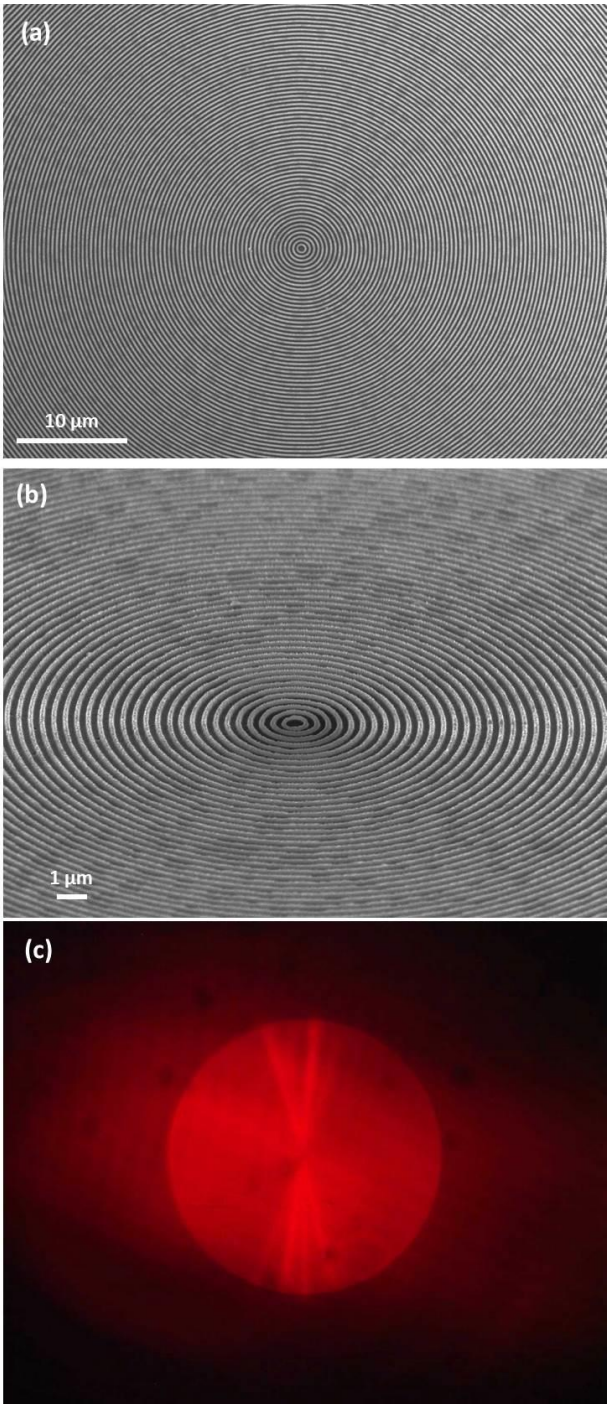

Figure 1 SEM images of the circular Bragg grating (a thin layer of PEDOT:PSS was spin-coated to avoid charge accumulation) when it was observed at (a) 0° and (b) 45°. (c) The far-field radiation pattern of the CQDs on the circular grating substrate under low excitation level. The diameter of the circular grating pattern is 188 µm.

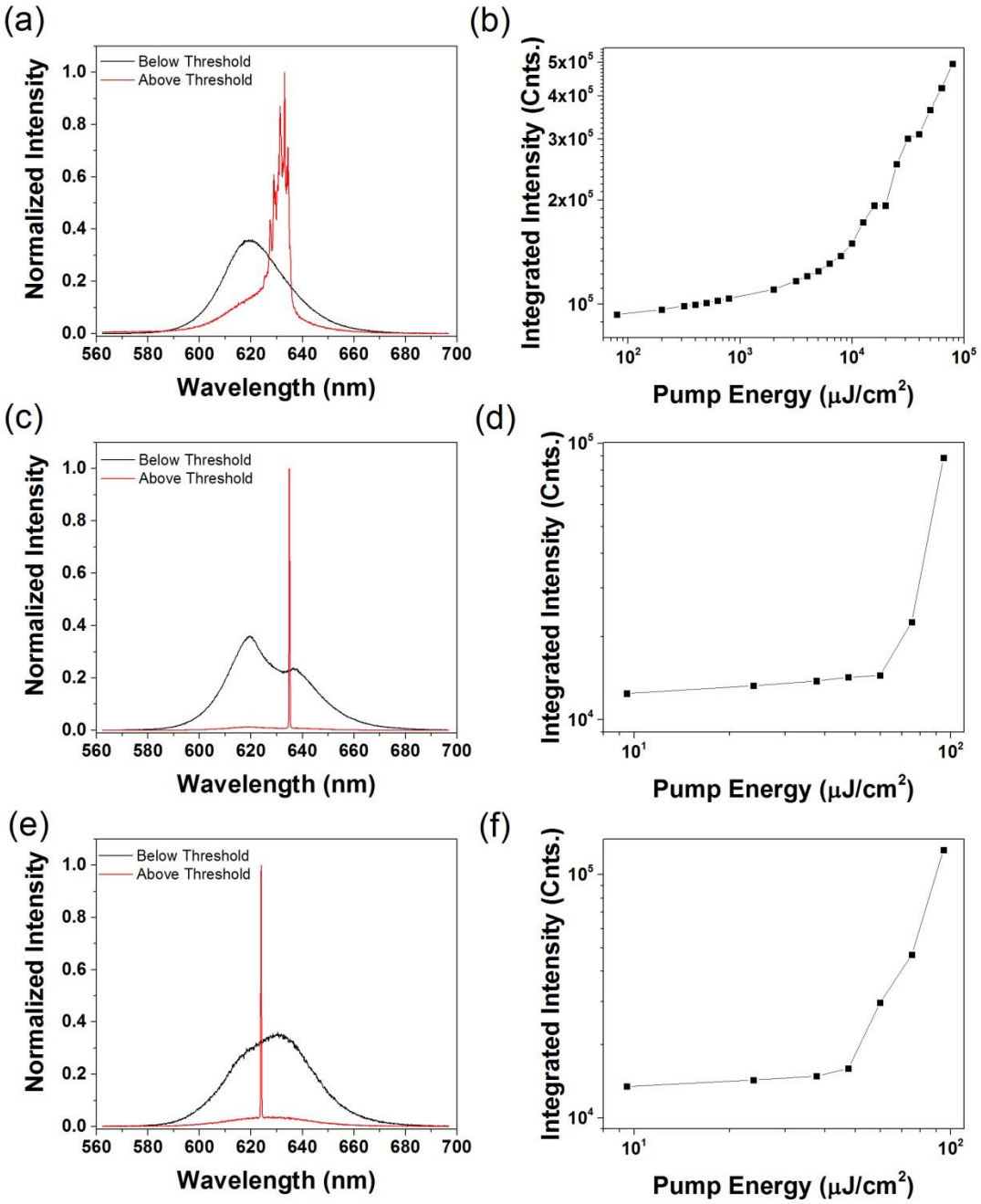

Figure 2 Characterization of the CQDs as gain medium and the CQD-CG-DFB lasers. (a) Normalized emission spectra of CQDs lying outside the circular gratings in the CQD film with the thickness of 247 nm below and above the ASE threshold. (b) The variation of integrated ASE intensity as a function of the pump energy. Normalized emission spectra of CQDs that coupled with the circular gratings below and above the lasing threshold and the integrated lasing intensity as a function of pump energy in the CQD film with the thickness of 247 nm (c, d), and 203 nm (e, f).

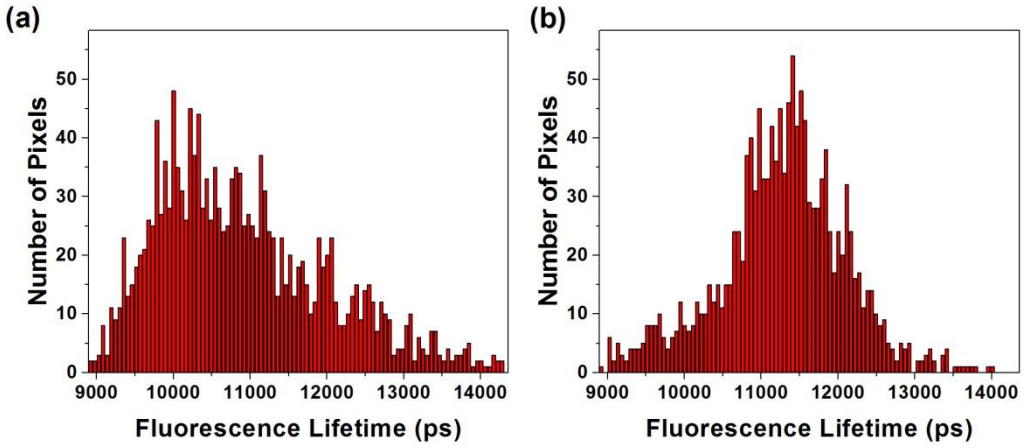

Figure 3 Fluorescence lifetime distribution CQDs in the mapping region that located outside (a) and within (b) the circular grating pattern.

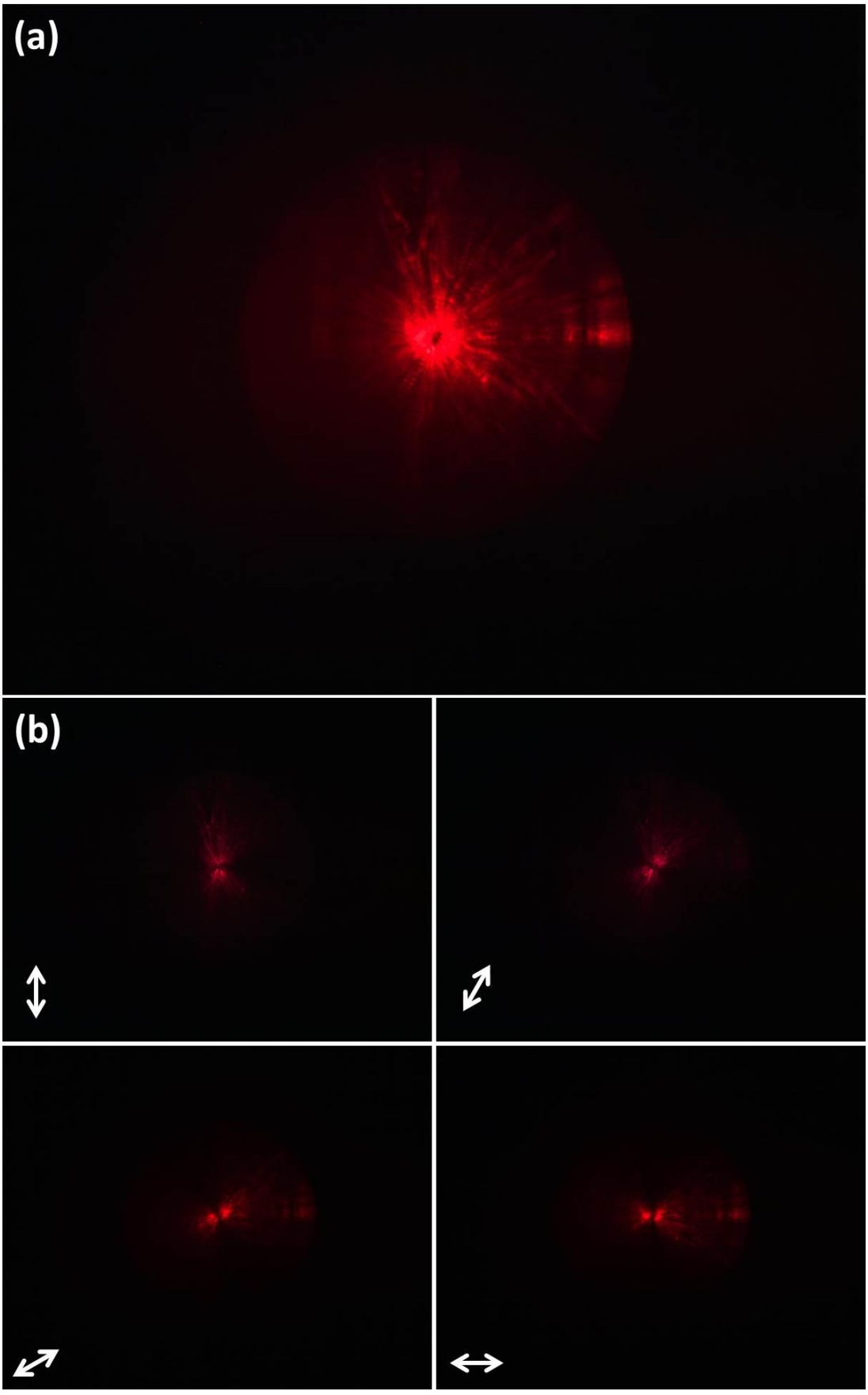
(a)
(b)

Figure 4 (a) Far-field radiation images that were captured via a CCD camera, when the CQD-CG-DFB laser was operating above the lasing threshold. (b) Variations of the far-field pattern CQD-CG-DFB laser as tuning the axis of the linear polarizer that the laser beam went through.

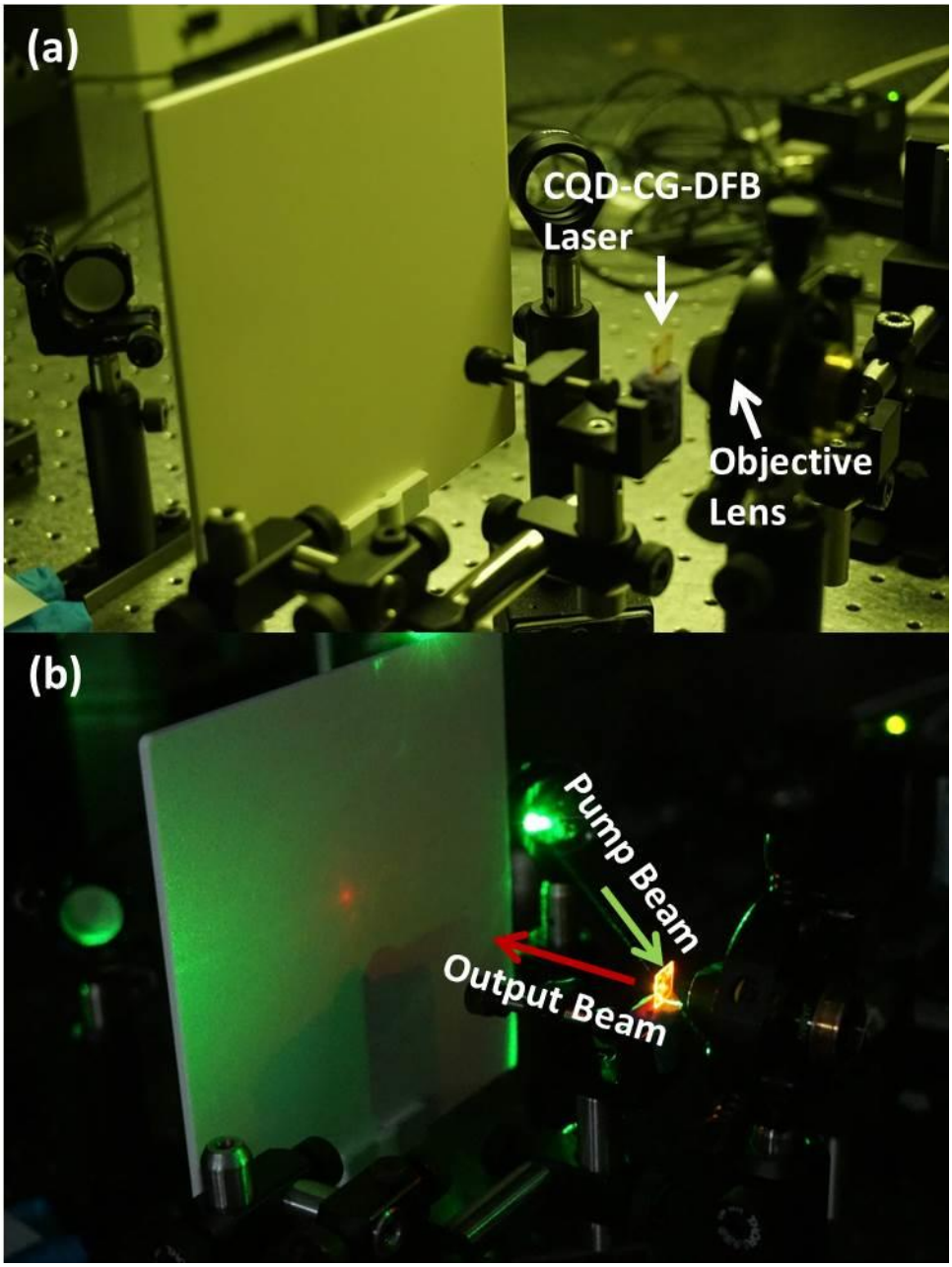

Figure 5 Demonstration of the spatial coherence of the output laser beam from the CQD-CG-DFB device. (a) The image of the measurement setup without optical pumping laser. (b) The image of the output beam when the CQD-CG-DFB laser was optically pumped above the lasing threshold.

REFERENCES

(1) Alivisatos, A. P. Birth of a Nanoscience Building Block. *ACS Nano* **2008,** *2*, 1514-1516.
(2) Rogach, A. Quantum Dots Still Shining Strong 30 Years On. *ACS Nano* **2014,** *8*, 6511-6512.

(3) Talapin, D. V.; Lee, J.-S.; Kovalenko, M. V.; Shevchenko, E. V. Prospects of Colloidal Nanocrystals for Electronic and Optoelectronic Applications. *Chemical Reviews* **2010,** *110*, 389-458.
(4) Coleman, J. J.; Bryce, A. C.; Jagadish, C. *Advances in Semiconductor Lasers*. Elsevier/Academic Press: 2012.
(5) Supran, G. J.; Shirasaki, Y.; Song, K. W.; Caruge, J.-M.; Kazlas, P. T.; Coe-Sullivan, S.; Andrew, T. L.; Bawendi, M. G.; Bulović, V. Qleds for Displays and Solid-State Lighting. *MRS Bulletin* **2013,** *38*, 703-711.
(6) Gaponenko, S.; Demir, H. V.; Seassal, C.; Woggon, U. Colloidal Nanophotonics: The Emerging Technology Platform. *Optics Express* **2016,** *24*, A430-A433.
(7) Klimov, V. I.; Mikhailovsky, A. A.; Xu, S.; Malko, A.; Hollingsworth, J. A.; Leatherdale, C. A.; Eisler, H.-J.; Bawendi, M. G. Optical Gain and Stimulated Emission in Nanocrystal Quantum Dots. *Science* **2000,** *290*, 314-317.
(8) Asada, M.; Miyamoto, Y.; Suematsu, Y. Gain and the Threshold of Three-Dimensional Quantum-Box Lasers. *IEEE Journal of quantum electronics* **1986,** *22*, 1915-1921.
(9) Klimov, V. I.; Mikhailovsky, A. A.; McBranch, D. W.; Leatherdale, C. A.; Bawendi, M. G. Quantization of Multiparticle Auger Rates in Semiconductor Quantum Dots. *Science* **2000,** *287*, 1011-1013.
(10) Klimov, V. I.; Ivanov, S. A.; Nanda, J.; Achermann, M.; Bezel, I.; McGuire, J. A.; Piryatinski, A. Single-Exciton Optical Gain in Semiconductor Nanocrystals. *Nature* **2007,** *447*, 441-446.
(11) Klimov, V. I. Spectral and Dynamical Properties of Multiexcitons in Semiconductor Nanocrystals. *Annu Rev Phys Chem* **2007,** *58*, 635-673.
(12) Dang, C.; Lee, J.; Breen, C.; Steckel, J. S.; Coe-Sullivan, S.; Nurmikko, A. Red, Green and Blue Lasing Enabled by Single-Exciton Gain in Colloidal Quantum Dot Films. *Nat Nano* **2012,** *7*, 335-339.
(13) Guzelturk, B.; Kelestemur, Y.; Gungor, K.; Yeltik, A.; Akgul, M. Z.; Wang, Y.; Chen, R.; Dang, C.; Sun, H.; Demir, H. V. Stable and Low-Threshold Optical Gain in Cdse/Cds Quantum Dots: An All-Colloidal Frequency up-Converted Laser. *Advanced Materials* **2015,** *27*, 2741-2746.
(14) Gao, Y.; Ta, V. D.; Zhao, X.; Wang, Y.; Chen, R.; Mutlugun, E.; Fong, K. E.; Tan, S. T.; Dang, C.; Sun, X. W., *et al.* Observation of Polarized Gain from Aligned Colloidal Nanorods. *Nanoscale* **2015,** *7*, 6481-6486.
(15) Kazes, M.; Lewis, D. Y.; Ebenstein, Y.; Mokari, T.; Banin, U. Lasing from Semiconductor Quantum Rods in a Cylindrical Microcavity. *Advanced Materials* **2002,** *14*, 317-321.
(16) Gao, Y.; Yu, G.; Wang, Y.; Dang, C.; Sum, T. C.; Sun, H.; Demir, H. V. Green Stimulated Emission Boosted by Nonradiative Resonant Energy Transfer from Blue Quantum Dots. *The Journal of Physical Chemistry Letters* **2016,** *7*, 2772-2778.
(17) Roh, K.; Dang, C.; Lee, J.; Chen, S.; Steckel, J. S.; Coe-Sullivan, S.; Nurmikko, A. Surface-Emitting Red, Green, and Blue Colloidal Quantum Dot Distributed Feedback Lasers. *Optics Express* **2014,** *22*, 18800-18806.
(18) Guilhabert, B.; Foucher, C.; Haughey, A. M.; Mutlugun, E.; Gao, Y.; Herrnsdorf, J.; Sun, H. D.; Demir, H. V.; Dawson, M. D.; Laurand, N. Nanosecond Colloidal Quantum Dot Lasers for Sensing. *Optics Express* **2014,** *22*, 7308-7319.
(19) Dang, C.; Lee, J.; Roh, K.; Kim, H.; Ahn, S.; Jeon, H.; Breen, C.; Steckel, J. S.; Coe-Sullivan, S.; Nurmikko, A. Highly Efficient, Spatially Coherent Distributed Feedback Lasers from Dense Colloidal Quantum Dot Films. *Applied Physics Letters* **2013,** *103*, 171104.
(20) Zavelani-Rossi, M.; Krahne, R.; Della Valle, G.; Longhi, S.; Franchini, I. R.; Girardo, S.; Scotognella, F.; Pisignano, D.; Manna, L.; Lanzani, G., *et al.* Self-Assembled Cdse/Cds Nanorod Micro-Lasers Fabricated from Solution by Capillary Jet Deposition. *Laser & Photonics Reviews* **2012,** *6*, 678-683.

(21) Nurmikko, A. What Future for Quantum Dot-Based Light Emitters? *Nat Nano* **2015,** *10*, 1001-1004.
(22) Erdogan, T.; Hall, D. G. Circularly Symmetric Distributed Feedback Semiconductor Laser: An Analysis. *J Appl Phys* **1990,** *68*, 1435-1444.
(23) Erdogan, T.; King, O.; Wicks, G. W.; Hall, D. G.; Anderson, E. H.; Rooks, M. J. Circularly Symmetric Operation of a Concentric-Circle-Grating, Surface- Emitting, Algaas/Gaas Quantum-Well Semiconductor Laser. *Applied Physics Letters* **1992,** *60*, 1921-1923.
(24) Erdogan, T.; Hall, D. G. Circularly Symmetric Distributed Feedback Laser: Coupled Mode Treatment of Te Vector Fields. *IEEE Journal of Quantum Electronics* **1992,** *28*, 612-623.
(25) Chen, Y.; Guilhabert, B.; Herrnsdorf, J.; Zhang, Y.; Mackintosh, A. R.; Pethrick, R. A.; Gu, E.; Laurand, N.; Dawson, M. D. Flexible Distributed-Feedback Colloidal Quantum Dot Laser. *Applied Physics Letters* **2011,** *99*, 241103.
(26) Chen, Y.; Li, Z.; Zhang, Z.; Psaltis, D.; Scherer, A. Nanoimprinted Circular Grating Distributed Feedback Dye Laser. *Applied Physics Letters* **2007,** *91*, 051109.
(27) Bae, W. K.; Kwak, J.; Lim, J.; Lee, D.; Nam, M. K.; Char, K.; Lee, C.; Lee, S. Multicolored Light-Emitting Diodes Based on All-Quantum-Dot Multilayer Films Using Layer-by-Layer Assembly Method. *Nano Lett* **2010,** *10*, 2368-2373.
(28) Wang, Y.; Ta, V. D.; Gao, Y.; He, T. C.; Chen, R.; Mutlugun, E.; Demir, H. V.; Sun, H. D. Stimulated Emission and Lasing from Cdse/Cds/Zns Core-Multi-Shell Quantum Dots by Simultaneous Three-Photon Absorption. *Advanced Materials* **2014,** *26*, 2954-2961.
(29) Cragg, G. E.; Efros, A. L. Suppression of Auger Processes in Confined Structures. *Nano Lett* **2010,** *10*, 313-317.
(30) Herrnsdorf, J.; Guilhabert, B.; Chen, Y.; Kanibolotsky, A. L.; Mackintosh, A. R.; Pethrick, R. A.; Skabara, P. J.; Gu, E.; Laurand, N.; Dawson, M. D. Flexible Blue-Emitting Encapsulated Organic Semiconductor Dfb Laser. *Optics Express* **2010,** *18*, 25535-25545.
(31) Joannopoulos, J. D.; Johnson, S. G.; Winn, J. N.; Meade, R. D. *Photonic Crystals: Molding the Flow of Light (Second Edition)*. Princeton University Press: 2011.
(32) Kopp, V. I.; Fan, B.; Vithana, H. K. M.; Genack, A. Z. Low-Threshold Lasing at the Edge of a Photonic Stop Band in Cholesteric Liquid Crystals. *Optics Letters* **1998,** *23*, 1707-1709.
(33) Bauer, C.; Giessen, H.; Schnabel, B.; Kley, E. B.; Schmitt, C.; Scherf, U.; Mahrt, R. A Surface-Emitting Circular Grating Polymer Laser. *Advanced Materials* **2001,** *13*, 1161-1164.
(34) Jordan, R. H.; Hall, D. G.; King, O.; Wicks, G.; Rishton, S. Lasing Behavior of Circular Grating Surface-Emitting Semiconductor Lasers. *Journal of the Optical Society of America B* **1997,** *14*, 449-453.